Molecular Cell
Article

The Eukaryotic Translation Initiation Factors eIF1 and eIF1A Induce an Open Conformation of the 40S Ribosome

Lori A. Passmore,[1] T. Martin Schmeing,[1] David Maag,[2,3] Drew J. Applefield,[2,4] Michael G. Acker,[2] Mikkel A. Algire,[2,5] Jon R. Lorsch,[2,*] and V. Ramakrishnan[1,*]
[1] MRC-Laboratory of Molecular Biology, Hills Road, Cambridge CB2 2QH, UK
[2] Department of Biophysics and Biophysical Chemistry, Johns Hopkins University School of Medicine, 725 N. Wolfe Street, Baltimore, MD 21205, USA
[3] Present address: Department of Neuroscience, Johns Hopkins University School of Medicine, 725 N. Wolfe Street, Baltimore, MD 21205, USA.
[4] Present address: LifeTech Research, Inc., 3962 Germantown Road, Suite 1A, Edgewater, MD 21037, USA.
[5] Present address: J. Craig Venter Institute, 9704 Medical Center Drive, Rockville, MD 20850, USA.
*Correspondence: jlorsch@jhmi.edu (J.R.L.), ramak@mrc-lmb.cam.ac.uk (V.R.)
DOI 10.1016/j.molcel.2007.03.018

SUMMARY

Initiation of translation is the process by which initiator tRNA and the start codon of mRNA are positioned in the ribosomal P site. In eukaryotes, one of the first steps involves the binding of two small factors, eIF1 and eIF1A, to the small (40S) ribosomal subunit. This facilitates tRNA binding, allows scanning of mRNA, and maintains fidelity of start codon recognition. Using cryo-EM, we have obtained 3D reconstructions of 40S bound to both eIF1 and eIF1A, and with each factor alone. These structures reveal that together, eIF1 and eIF1A stabilize a conformational change that opens the mRNA binding channel. Biochemical data reveal that both factors accelerate the rate of ternary complex (eIF2•GTP•Met-tRNA$_i^{Met}$) binding to 40S but only eIF1A stabilizes this interaction. Our results suggest that eIF1 and eIF1A promote an open, scanning-competent preinitiation complex that closes upon start codon recognition and eIF1 release to stabilize ternary complex binding and clamp down on mRNA.

INTRODUCTION

Translation of mRNA by ribosomes can be divided into four phases: initiation, elongation, termination, and recycling. Although most of these steps are highly conserved between prokaryotes and eukaryotes, initiation is much more complex in eukaryotes. During translation initiation, active 80S complexes are formed when small (40S) and large (60S) ribosomal subunits assemble on mRNA, with the start codon and a methionyl initiator tRNA (Met-tRNA$_i^{Met}$) in the peptidyl (P) site. In eukaryotes, at least 12 initiation factors (eIFs), composed of ~28 polypeptides, are involved in this process, whereas only three factors are required in prokaryotes (Kapp and Lorsch, 2004b). It is thought that some initiation factors could carry out their functions by mediating conformational changes in the 40S subunit, for example to assist mRNA or tRNA binding. However, the nature of such conformational changes is unknown.

A variety of in vitro and in vivo experiments have helped to establish the roles of the initiation factors (reviewed in Kapp and Lorsch [2004b]). In a reconstituted translation initiation system using purified yeast components and an uncapped, unstructured mRNA (Algire et al., 2002), eIF1 and eIF1A are sufficient to promote assembly of a 43S•mRNA complex from the 40S subunit, mRNA, and ternary complex (eIF2•GTP•Met-tRNA$_i^{Met}$). The 43S complex is thought to scan along mRNA until it recognizes the initiation codon, which induces the dissociation of eIF1 and subsequent release of phosphate by the GTPase eIF2 (Algire et al., 2005; Maag et al., 2006). This irreversible step is facilitated by the activity of eIF5, a GTPase activating protein (GAP) (Das et al., 2001; Paulin et al., 2001; Algire et al., 2005). Finally, eIF5B promotes initiation factor dissociation and subunit joining to form an active 80S ribosome containing initiator tRNA within the P site, base paired with the AUG start codon. In vivo, an additional multisubunit factor, eIF3, plays a role in 43S complex formation and, along with eIF4F, eIF4B, and PAB, is required for loading mRNAs onto the preinitiation complex.

eIF1 and eIF1A are small proteins (12 and 17 kDa, respectively) that bind cooperatively to the 40S subunit with high affinity (Maag and Lorsch, 2003), are essential for viability in yeast, and are highly conserved among all eukaryotes (Hershey and Merrick, 2000; Kapp and Lorsch, 2004b). They are required for formation of a 43S•mRNA complex that is competent for scanning and accurate recognition of the initiation codon, possibly by affecting the equilibrium between a "closed," scanning-incompetent

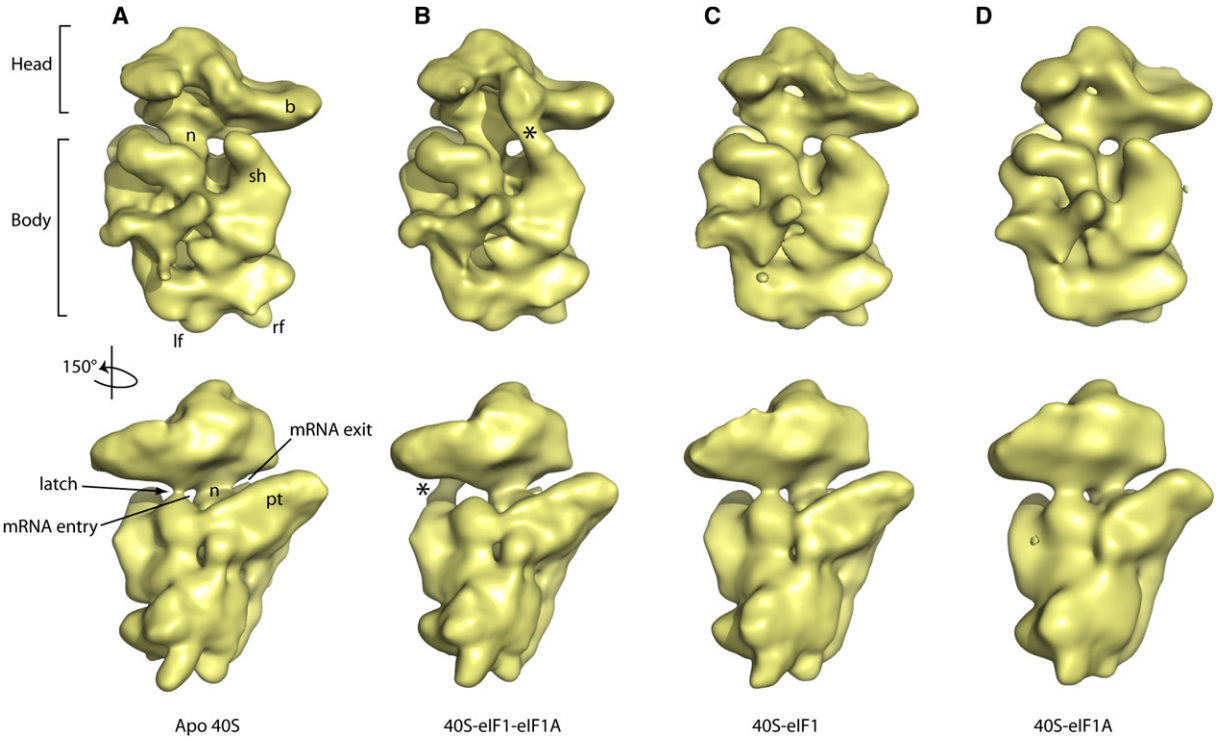

Figure 1. Structures of Yeast 40S Preinitiation Complexes

Cryo-EM reconstructions of (A) apo 40S, (B) 40S-eIF1-eIF1A, (C) 40S-eIF1, and (D) 40S-eIF1A. The 40S subunit is viewed from the solvent side (top) and the 60S interface side (bottom). Small ribosomal subunit landmarks are shown on apo 40S. Abbreviations: b, beak; n, neck; sh, shoulder; pt, platform; lf, left foot; and rf, right foot. The connection between shoulder and head induced by binding of eIF1 and eIF1A is highlighted by an asterisk in (B).

state and an "open," scanning-competent state (Pestova et al., 1998, 2001; Pestova and Kolupaeva, 2002; Maag et al., 2005). eIF1 and eIF1A act synergistically and have also been reported to assist ternary complex binding (Chaudhuri et al., 1999; Algire et al., 2002; Majumdar et al., 2003; Olsen et al., 2003; Singh et al., 2004).

NMR or X-ray crystal structures have been determined for these and many other initiation factors in isolation (Sonenberg and Dever, 2003), but they have offered limited understanding of eIF function(s) within the context of the 40S subunit and/or 80S ribosome. To understand the initial steps of eukaryotic translation, we have determined structures of the yeast 40S ribosomal subunit in complex with eIF1 and eIF1A. We show that the binding of these small factors results in conformational changes in the 40S subunit. These changes help rationalize how the 40S initiation complex binds ternary complex and mRNA and positions the start codon in its active site. We suggest that the 40S-eIF1-eIF1A structure represents an open, scanning-competent form of the initiation complex.

RESULTS AND DISCUSSION

Cryo-EM Reconstruction of Yeast 40S Bound to eIF1 and eIF1A

To understand how the small initiation factors eIF1 and eIF1A help mediate translation initiation, we determined the structure of the 40S ribosomal subunit alone and bound to eIF1 and eIF1A by using cryo-electron microscopy (cryo-EM). 40S subunits purified from *Saccharomyces cerevisiae* were previously shown to be active in binding these factors and in forming functional 80S initiation complexes (Algire et al., 2002). Moreover, it has been shown that the binding of eIF1 and eIF1A to the 40S subunit is thermodynamically coupled and that they bind with high affinity in vitro (1.7 nM and 6.1 nM, respectively [Maag and Lorsch, 2003]). For cryo-EM studies, we used 50–75 nM 40S and a 5-fold molar excess of each factor and therefore expect that most of the 40S will be present as a 40S-eIF1-eIF1A complex. Empty 40S and 40S-eIF1-eIF1A cryo-EM reconstructions were refined to resolutions of ~21 and 22 Å, respectively (at 0.5 FSC; ~16 Å and 17 Å at 0.143 FSC).

The reconstruction of empty 40S (Figure 1A) reveals the classical small ribosomal subunit structure (Spahn et al., 2001a, 2001b, 2004b). However, the 40S-eIF1-eIF1A reconstruction reveals striking differences in the conformation of the 40S subunit (Figure 1B and Movies S1–S4 in the Supplemental Data available with this article online). Specifically, we observe a new connection between the head and shoulder on the solvent side. In addition, the "latch" of the mRNA entry channel is closed in empty 40S but is not visible in the 40S-eIF1-eIF1A structure. This latch is a noncovalent interaction between rRNA elements in the body

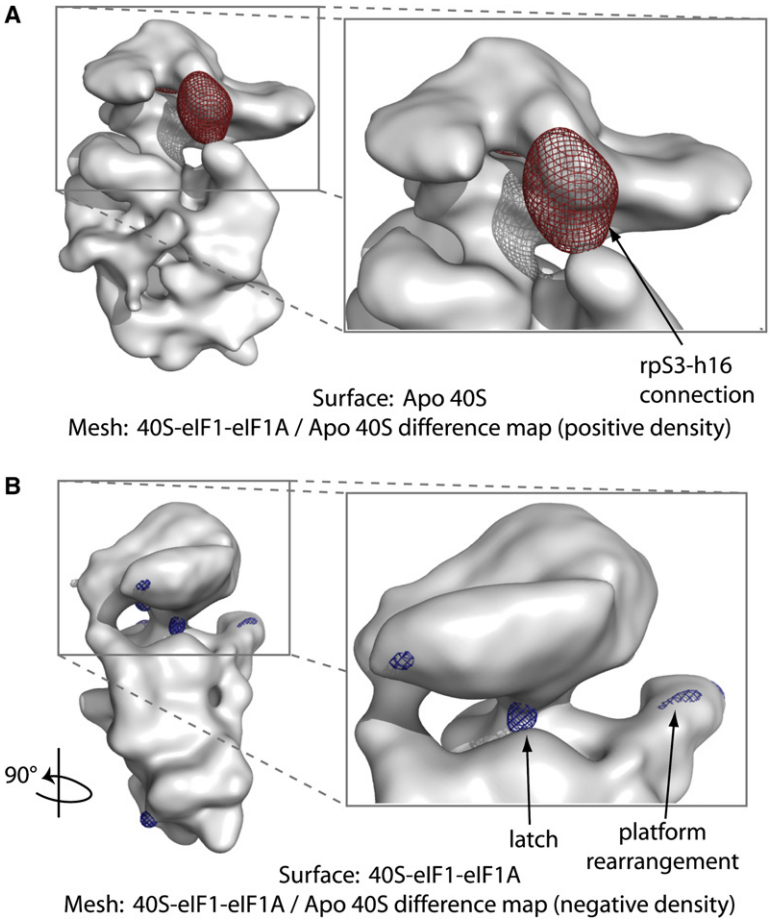

Figure 2. Difference Density Maps between 40S-eIF1-eIF1A and Apo 40S

Difference maps were calculated by subtracting the apo 40S density from the 40S-eIF1-eIF1A map.

(A) Positive difference density (contoured at a sigma level of 20) is shown in red mesh overlaid on the apo 40S map (gray surface).

(B) Negative difference density (contoured at a sigma level of −12) is shown in blue mesh overlaid on the 40S-eIF1-eIF1A map (gray surface).

and head that is proposed to clamp around the incoming mRNA (Frank et al., 1995; Schluenzen et al., 2000). These rearrangements are clearly visible in difference maps (Figure 2).

To evaluate the significance of these conformational changes, we performed several additional experiments. First, we split each data set into two and calculated two independent apo 40S maps and two independent 40S-eIF1-eIF1A maps by separately refining each data set against a common model. We then calculated two independent difference maps. As shown in Figure S1, these independent difference maps correlate very well in the regions of new head-shoulder connection and mRNA entry channel latch, confirming the significance of these conformational changes.

To determine the statistical significance of the conformational changes we observe upon eIF1 and eIF1A binding in a more quantitative way, we performed a Student's t test on the maps. To determine the variance, we either used four independent maps calculated from each data set with a method similar to that described above (Figure S2) or used the bootstrap method described by Penczek et al. (2006) (Figure S3). The t maps also demonstrate that the differences we observe (head-shoulder connection and mRNA entry channel latch) are highly significant ($p << 0.0001$). As shown in the animations in Movies S1–S4, there appears to be smaller movements in other regions of the 40S subunit upon eIF1 and eIF1A binding, including changes in the orientations of the right foot, beak, and platform, but their significance is unclear.

Structures of 40S-eIF1 and 40S-eIF1A Complexes

To better understand how eIF1 and eIF1A each influence the conformational changes we observe in the 40S-eIF1-eIF1A structure, we determined cryo-EM reconstructions of the 40S subunit bound to each factor individually. The reconstructions of 40S-eIF1 and 40S-eIF1A were refined to resolutions of 24 and 25 Å, respectively (by 0.5 FSC criteria; 19 and 20 Å at 0.143 FSC). The structures of 40S-eIF1 and 40S-eIF1A are similar to that of empty 40S (Figures 1C and 1D). In particular, the striking connection between the shoulder and head observed in the 40S-eIF1-eIF1A complex is clearly absent and the mRNA entry channel is closed. However, the 40S-eIF1A structure appears to exhibit small differences from empty 40S, including a tilted beak and strong density for the mRNA entry channel latch (Figure 1D). Because biochemical studies have shown that eIF1 and eIF1A act synergistically

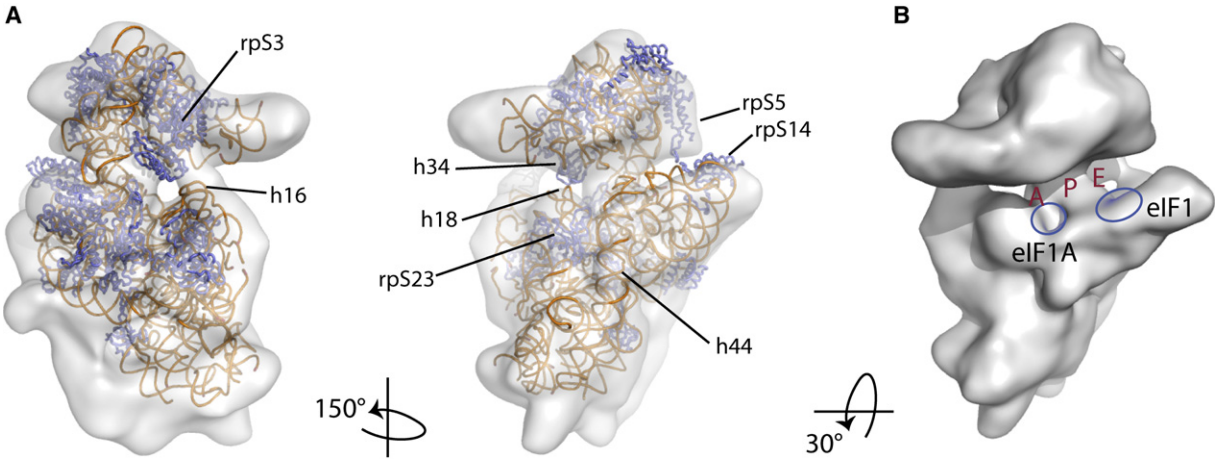

Figure 3. Mapping of 18S rRNA, 40S Ribosomal Proteins, eIF1, and eIF1A in the 40S-eIF1-eIF1A Cryo-EM Map

(A) The docked molecular model of the yeast 40S subunit is shown for the 40S-eIF1-eIF1A cryo-EM map (transparent surface). 18S rRNA is shown in orange, and ribosomal proteins are shown in purple. Several important rRNA helices and ribosomal proteins are labeled. Note that the mRNA entry and exit channels (h18-h34 and rpS5-rpS14) are open in our structure but closed in the docked 40S model.

(B) The approximate binding sites for eIF1A (Carter et al., 2001) and eIF1 (Lomakin et al., 2003) (blue), and the A, P, and E sites, (red) are indicated on the surface of 40S-eIF1-eIF1A.

(Pestova et al., 1998; Maag and Lorsch, 2003; Majumdar et al., 2003), it is not surprising that eIF1 or eIF1A alone does not induce a major conformational change and that both factors are required to stabilize the 40S-eIF1-eIF1A structure.

Interpretation of the EM Maps Using a 40S Model

A molecular model for the evolutionarily conserved core of the *S. cerevisiae* 80S ribosome is available (Spahn et al., 2001a, 2004a). This model was constructed by using cryo-EM in combination with homology modeling and is based on the atomic structures of the prokaryotic 30S and 50S subunits. To facilitate interpretation of our cryo-EM reconstructions, we docked the coordinates of the 40S portion of this model into our maps as a rigid body (Figure 3A and Movie S5). There are some discrepancies between the docked model and our maps that are probably due to conformational changes that occur upon 80S formation. For example, the platform appears to be in a more extended position in all of our 40S maps (including empty 40S), compared to 60S-bound 40S (Figure 3A). A similar observation has been made for isolated versus 50S-bound 30S and likely reflects structural flexibility of the isolated subunit (Lata et al., 1996; Gabashvili et al., 1999). However, most of the docked 40S subunit fits well with our maps (with a crosscorrelation coefficient of 0.78), allowing us to assign specific rRNA helices and ribosomal proteins to the regions in which conformational changes occur, as discussed below.

Entry Channel Latch

The mRNA entry channel latch is formed by a noncovalent interaction between 18S rRNA helices 18 and 34 (Frank et al., 1995; Schluenzen et al., 2000; Wimberly et al., 2000; Spahn et al., 2001a; Yusupova et al., 2001). The latch is open in the 40S-eIF1-eIF1A structure (Figure 1B and Movie S2), making the mRNA entry channel more accessible. This would allow mRNA to dock into the mRNA binding channel directly in the initiation complex, instead of threading through a small tunnel (Lata et al., 1996; Spahn et al., 2004b). Indeed, it is thought that the latch must open to allow mRNA binding, because in vivo, a large protein complex (eIF4F) is bound to the 5′ end of mRNA. The latch is proposed to clamp around the mRNA, either after start codon recognition or after subunit joining, to trap the mRNA on the ribosome, preventing mRNA dissociation and facilitating processivity (Lata et al., 1996; Schluenzen et al., 2000; Yusupova et al., 2001). In agreement with this, in apo 40S, 40S-eIF1, and 40S-eIF1A, the latch is closed (Figure 1). Density for the latch appears more pronounced in 40S-eIF1A (Figure 1D), suggesting that the h18-h34 connection may be stronger when eIF1A is bound. Because eIF1 dissociates after start codon recognition, perhaps eIF1A, when present without eIF1, helps the 40S subunit to clamp down on the mRNA, holding it in position in preparation for 60S subunit joining.

Helix 16-rpS3 Interaction

As mentioned above, together, eIF1 and eIF1A promote the formation of a new connection between the head and shoulder on the solvent side of the 40S subunit (Figures 1B and 2A and Movie S1). This striking new connection is likely mediated by an interaction between 18S rRNA helix 16 and the ribosomal protein rpS3 (Figure 3A). In agreement with this, the beak (which contains rpS3) exhibits a slightly altered conformation (Movie S3). In apo 40S, helix 16 points into the solvent (Figure 1A) while rpS3 stabilizes the closed position of the mRNA latch through interactions with helix 34. We propose that the

new h16-rpS3 connection in the 40S-eIF1-eIF1A structure stabilizes the head in a position that prevents the mRNA latch from reforming.

mRNA Exit Channel

mRNA leaves the ribosome through the mRNA exit channel, formed by interaction of rpS14 and rpS5 (Yusupova et al., 2001). The exit channel is closed in yeast 80S cryo-EM maps (Spahn et al., 2001a) but open in our isolated 40S structures (Figures 1 and 3A). The open mRNA exit channel and movement of the platform away from the 40S body acts to open the mRNA binding channel and could facilitate tRNA and/or mRNA binding.

eIF1 and eIF1A Binding Sites

Due to the small sizes of eIF1 and eIF1A (12 and 17 kDa, respectively) and the rearrangements in the 40S subunit that occur upon their binding, it is difficult at this resolution to confidently identify densities directly attributable to eIF1 and/or eIF1A. (eIF1 and eIF1A account for only ~2% of the total mass of the 40S-eIF1-eIF1A complex.) New features in density maps can be caused by conformational changes or by the addition of new proteins. Thus, attempts to interpret factor/ligand densities in difference maps when significant conformational changes are also present can lead to spurious conclusions (for example, see McCutcheon et al. [1999] and Dallas and Noller [2001]). So far, our attempts to label eIF1 and eIF1A with a gold cluster to facilitate visualization of the factors in complex with the 40S subunit have been unsuccessful due to aggregation of the gold-labeled factors and reduced 40S binding. However, the binding positions of both factors can be approximated by using additional data.

eIF1 is required for maintaining the fidelity of start site selection and preventing initiation from occurring at non-AUG codons or AUG codons in poor context (Yoon and Donahue, 1992; Pestova and Kolupaeva, 2002; Valasek et al., 2004). Thus, eIF1 is proposed to monitor base pairing between mRNA and Met-tRNA$_i^{Met}$. Hydroxyl-radical probing has mapped the binding site of eIF1 to the interface side of the 40S subunit, between the platform and initiator tRNA, in a similar position to the C-terminal domain of prokaryotic IF3 (Figure 3B; McCutcheon et al., 1999; Dallas and Noller, 2001; Lomakin et al., 2003). Although this is close to the ribosomal P site, eIF1 would not be able to directly monitor codon-anticodon base pairing from this position. Instead, it was hypothesized that eIF1 indirectly monitors start codon recognition by influencing the conformation of the platform and the positions of mRNA and tRNA (Lomakin et al., 2003). Intriguingly, we observe statistically significant difference density on the platform, within the vicinity of the proposed eIF1 binding site (Figure 2B and Figures S2 and S3), which could be the result of eIF1 binding.

eIF1A, which is homologous to the prokaryotic initiation factor IF1, also facilitates 43S complex formation and scanning (Pestova et al., 1998; Fekete et al., 2005). It helps to maintain the fidelity of start codon recognition, likely through an interaction with eIF5 and by stabilizing the open, scanning-competent 40S conformation until the start codon is identified (Maag et al., 2006). A crystal structure of IF1 bound to the prokaryotic small (30S) ribosomal subunit showed that IF1 binds in the A site, blocking initiator tRNA from binding in this position (Carter et al., 2001). eIF1A is expected to bind in a similar position to IF1 (Figure 3B).

When the proposed binding sites of eIF1 and eIF1A are mapped onto the 40S-eIF1-eIF1A structure (Figure 3B), it is clear that the factor binding sites are remote from many of the observed conformational changes. Therefore, many of the conformational changes, including the new h16-rpS3 connection on the solvent side, are expected to be allosteric changes caused by eIF1 and eIF1A binding on the interface side.

eIF1 and eIF1A Affect Ternary Complex Binding

Our observation that eIF1 and eIF1A facilitate an opening of the mRNA binding channel suggests a molecular mechanism for how these factors could enhance the binding of ternary complex to the small ribosomal subunit (Kapp and Lorsch, 2004b). To test the hypothesis that eIF1 and eIF1A enhance ternary complex loading by altering the conformation of the 40S subunit, we examined the effects of these factors on the kinetics of ternary complex binding and dissociation by using a reconstituted yeast translation initiation system (Algire et al., 2002).

The observed pseudo-first-order rate constant (k_{obs}) for ternary complex binding to the 40S subunit displays a linear dependence on 40S subunit concentration (Figures 4A and 4B). From these data, we can calculate a second-order rate constant for the binding of ternary complex to the 40S subunit (k_{on}; for a simple binding model $k_{obs} = k_{on}[40S] + k_{off}$ [Johnson, 1992]). In the presence of saturating concentrations of eIF1, eIF1A, and a minimal model mRNA containing an AUG codon, ternary complex binds to the 40S subunit with a k_{on} of 3.8×10^7 M^{-1} s^{-1}, near the diffusion-controlled limit (Figure 4A). Although it is theoretically possible to calculate the rate constant for dissociation (k_{off}) from these data (Table 1), this requires extrapolation to zero 40S subunit concentration, making the calculated values extremely sensitive to small degrees of experimental error. We therefore measured k_{off} directly (Figure 4C). In the presence of eIF1, eIF1A, and mRNA, ternary complex is bound to the 40S subunit very tightly, with a k_{off} of 1.4×10^{-6} s^{-1} and a K_d (calculated as k_{off}/k_{on}) of 3.7×10^{-5} nM.

In the absence of either eIF1A or mRNA, k_{on} is decreased 10,000-fold to 2820 and 4200 M^{-1} s^{-1}, respectively (Table 1 and Figure 4B). The fact that these values are significantly below the diffusion limit suggests that a first-order process such as a conformational change is at least partially rate limiting for ternary complex binding under these conditions (Johnson, 1992). eIF1A and mRNA also significantly decrease k_{off} and K_d (Table 1 and Figure 4C), indicating that both eIF1A and mRNA stabilize the binding of ternary complex to the 40S subunit.

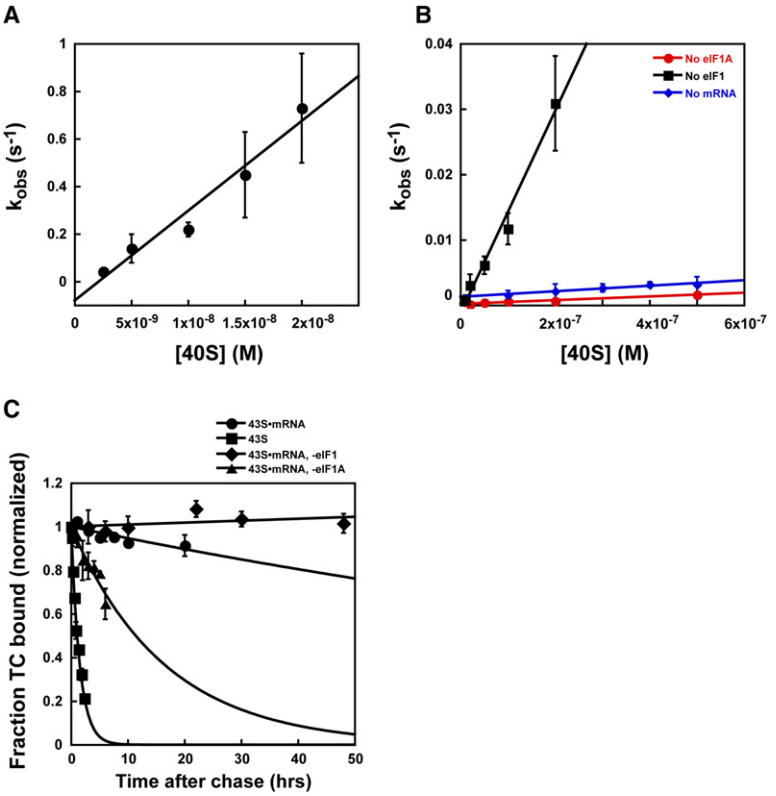

Figure 4. The Effects of eIF1 and eIF1A on the Kinetics and Thermodynamics of Ternary Complex Binding to the 40S Subunit

All experiments were carried out at least three times. The values depicted are means of replicate experiments and the error bars are mean deviations.

(A) In the presence of saturating eIF1, eIF1A, and an AUG-containing mRNA, ternary complex binds to the ribosome with a second-order rate constant near the diffusion limit (3.8×10^7 M^{-1} s^{-1}).

(B) Omission of eIF1, eIF1A, or mRNA significantly decreases k_{on} for ternary complex binding to the 40S subunit.

(C) Omission of eIF1A or mRNA increases the rate constant for dissociation of ternary complex from the 40S subunit. In contrast, omission of eIF1 stabilizes ternary complex binding.

Similar to the effects of eIF1A and mRNA, eIF1 increases k_{on}, albeit to a smaller extent (245-fold, from 1.55×10^5 to 3.8×10^7 M^{-1} s^{-1}). In contrast to eIF1A and mRNA, however, eIF1 increases k_{off} from $<5 \times 10^{-7}$ to 1.4×10^{-6} s^{-1} (Figure 4C). This observation resolves seemingly conflicting observations in previous reports that eIF1 enhances ternary complex binding to the preinitiation complex but is also released from the complex upon start codon recognition (Algire et al., 2002; Maag et al., 2005). It is not possible for eIF1 to stabilize 43S•mRNA complex formation if its own affinity for the complex is weaker after ternary complex binding than before. The data presented here indicate that the effect of eIF1 on ternary complex binding to the 40S subunit is kinetic, with no stabilization of the interaction, resolving the apparent paradox. Instead, the release of eIF1 from the complex upon start codon recognition would serve to further strengthen the interaction between the ternary complex and the ribosome.

Together with our cryo-EM reconstructions, these biochemical data suggest that eIF1 and eIF1A work together to facilitate a conformational change in the 40S ribosomal subunit that significantly accelerates ternary complex loading. eIF1A plays an additional role by stabilizing ternary complex once it is bound.

Conformational Changes in Other Initiation Complexes: A Conserved Mechanism

Initiation of translation can proceed via the canonical pathway described above or via an alternative pathway where sequences in the 5′UTR of the mRNA direct the 40S subunit to assemble on a start codon with reduced or no

Table 1. Kinetic and Thermodynamic Parameters for Ternary Complex Binding to 40S Subunits

	k_{on} (M^{-1} s^{-1})	k_{off} (s^{-1})	$K_d^{calculated}$ (nM)[a]	$K_d^{measured}$ (nM)[c]
40S•1•1A	4200	1.8×10^{-4}	43	54[b]
40S•1•1A•mRNA	3.8×10^7	1.4×10^{-6}	3.7×10^{-5}	≤1
40S•1•mRNA	2820	1.7×10^{-5}	6	18
40S•1A•mRNA	1.55×10^5	$<5 \times 10^{-7}$	$<3 \times 10^{-3}$	≤1

[a] Calculated from k_{off}/k_{on}.
[b] From Maag et al. (2005).
[c] Measured using the native gel assay as described in Maag et al. (2005).

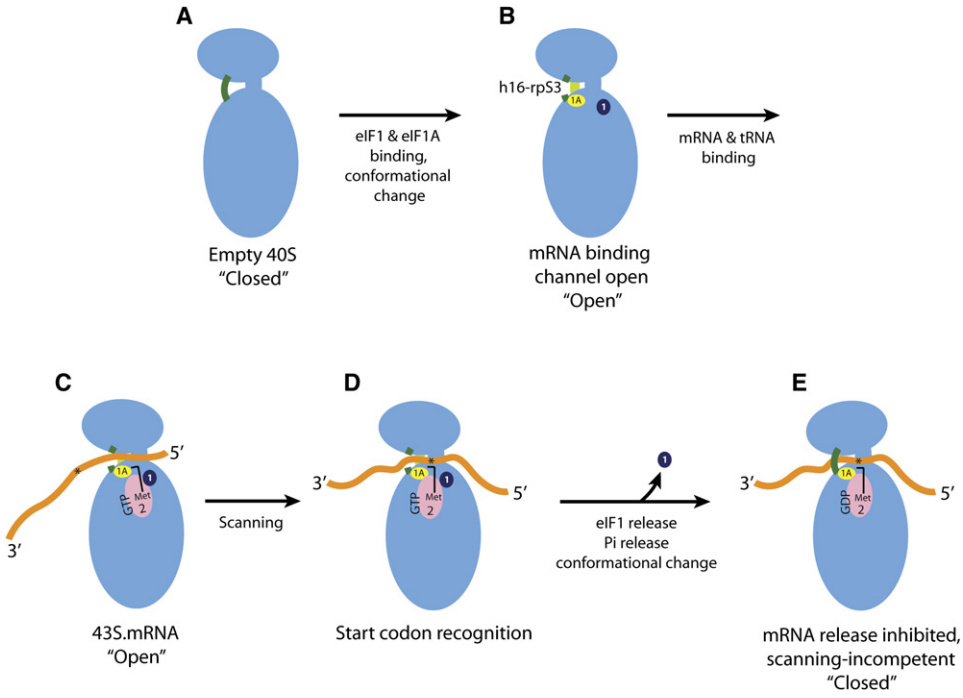

Figure 5. Model for the Functions of eIF1 and eIF1A in Eukaryotic Translation Initiation

(A) Empty 40S (blue) adopts a closed conformation with a closed mRNA entry channel latch (dark green).

(B) Upon eIF1 and eIF1A binding, a conformational change in the 40S subunit stabilizes the latch in an open position. This conformational change involves the formation of a new connection between h16 and rpS3 on the 40S solvent side (light green).

(C) The open conformation facilitates mRNA (orange) and ternary complex (pink) binding.

(D) eIF1 and eIF1A hold the mRNA binding channel open to allow scanning of the mRNA until a start codon (asterisk) is recognized.

(E) Upon start codon recognition, eIF1 and Pi (from the hydrolysis of GTP by eIF2) are released and a conformational change occurs to prevent further scanning. This closed complex likely has closed mRNA entry and exit channels, which clamp down on the mRNA, holding it in position until the 60S subunit joins and translation can begin. Note, for the sake of clarity, some steps are not shown.

dependence on initiation factors. These structured RNA sequences—internal ribosomal entry sites (IRESs)—are found in some viral and cellular RNAs and are used to "hijack" the host cell's translational apparatus (Bushell and Sarnow, 2002). Cryo-EM reconstructions have been determined for the 40S subunit bound to the hepatitis C virus (HCV) and cricket paralysis virus (CrPV) IRES sequences (Spahn et al., 2001b, 2004b).

Intriguingly, some of the IRES-induced conformational changes in both 40S-HCV IRES and 40S/80S-CrPV IRES reconstructions bear resemblance to those seen upon binding of eIF1 and eIF1A. In particular, both IRESs appear to induce an open mRNA entry channel latch and the formation of a bridge between the head and shoulder (h16-rpS3), suggesting that these are probably general features of translation initiation. It is likely that the h16-rpS3 and h18-h34 conformational changes are linked and the h16-rpS3 interaction stabilizes the open latch.

Although both canonical and IRES initiation complexes have changes in the shapes of the beak and platform, only the IRES structures show a strong rotation of the head compared to empty 40S (Spahn et al., 2001b, 2004b). Because IRES sequences contain the coding mRNA and directly place the start codon in the P site, it is possible that this head rotation occurs in response to start codon recognition and may prepare the 40S subunit for association with the large subunit (Spahn et al., 2004b). Notably, after 40S-CrPV joins the 60S subunit to form 80S-CrPV, the head is no longer rotated.

Model for eIF1 and eIF1A Function

Here, we have shown that eIF1 and eIF1A together mediate a conformational change in the 40S subunit that opens the mRNA binding channel and forms a new h16-rpS3 connection on the solvent side. This conformational change appears to be a fundamental requirement for translation initiation because it is also induced by IRESs. Because both eIF1 and eIF1A are required for the full conformational change, our results provide a mechanistic basis for earlier observations that eIF1 and eIF1A act cooperatively and interact (directly or indirectly) on the ribosome (Pestova et al., 1998; Maag and Lorsch, 2003; Majumdar et al., 2003). We propose that binding of eIF1 and eIF1A would thus convert the closed empty 40S structure into an open, scanning-competent preinitiation complex (Figure 5). The existence of such an open form has been proposed from biochemical experiments but has never been visualized (Pestova and Kolupaeva, 2002;

Maag et al., 2006). The open structure would (1) allow mRNA to bind within the mRNA binding channel with its open latch (Spahn et al., 2004b) (2) accelerate ternary complex binding (Figure 4), and (3) facilitate scanning by holding the mRNA binding channel open until a start codon is recognized.

Our results are also consistent with biochemical experiments suggesting that eIF1 influences start codon recognition through an indirect mechanism by affecting the positions of the platform, mRNA, and/or tRNA (Lomakin et al., 2003). It has been suggested that eIF1 antagonizes the closed, scanning-incompetent structure of the initiation complex that forms upon recognition of the start codon (Pisarev et al., 2006). In agreement with this, eIF1 is released upon start codon recognition (Maag et al., 2005), and 43S•mRNA complexes formed in the absence of eIF1 are unable to scan along mRNA (Pestova and Kolupaeva, 2002). The 40S-eIF1A reconstruction appears to have increased density for the closed mRNA entry channel latch, similar to the latch in an 80S structure. Upon start codon recognition, eIF1 release would relieve eIF1's antagonistic effect on the closed, scanning-incompetent form and allow the initiation complex to clamp down on the mRNA, holding it in place and priming the 40S subunit for interaction with the 60S subunit.

Similarly, some of the conformational changes induced by IF1 (the prokaryotic homolog of eIF1A) may organize the 30S subunit in preparation for association with the large subunit. IF1 induces long-range conformational changes in the 30S subunit, including tilting of the head, shoulder, and platform toward the A site and changes in the conformation of helix 44 (Carter et al., 2001). Thus, our model agrees well with a model for prokaryotic translation initiation where eIF1/IF3 antagonize subunit joining (by mediating conformational changes or directly blocking large subunit binding) while eIF1A/IF1—which remain bound to the small subunit after eIF1/IF3 dissociation—prepare the initiation complex for subunit joining after mRNA and tRNA binding (Maag et al., 2005; Antoun et al., 2006).

In this study, we used a reconstituted translation initiation system to demonstrate that an important conformational change is triggered by eIF1 and eIF1A in the early stages of translation initiation. Biochemical studies have shown that other rearrangements occur during initiation, for example upon start codon recognition (Algire et al., 2002; Pestova and Kolupaeva, 2002; Maag et al., 2005, 2006; Pisarev et al., 2006). The combination of our defined canonical translation initiation system and cryo-EM will enable us to further investigate the molecular mechanisms that accompany the steps of initiation, including mRNA binding, start codon recognition, and initiation factor release.

EXPERIMENTAL PROCEDURES

Purification of the 40S Subunit and Initiation Factors

eIF1 and eIF1A were overexpressed in *E. coli* and purified by using the IMPACT system (NEB) as previously described (Algire et al., 2002). His-tagged eIF2 was purified from *S. cerevisiae* strain GP3511 as described (Algire et al., 2002). Small ribosomal subunits were purified from *S. cerevisiae* strain YAS2488 as described (Maag et al., 2006). Initiator methionyl-tRNA and a minimal model mRNA were synthesized and purified as described (Kapp and Lorsch [2004a] and Lorsch and Herschlag [1999], respectively).

Cryo-EM and Image Processing

40S subunits were incubated on ice at a concentration of 500–750 nM with a 5-fold molar excess of each of eIF1 and eIF1A (for the 40S-eIF1-eIF1A complex) or a 10-fold molar excess of one of the factors (for the 40S-eIF1 and 40S-eIF1A complexes) in 20 mM HEPES-KOH (pH 7.4), 100 mM potassium acetate, 2.5 mM magnesium acetate, and 2 mM DTT. Samples were diluted to a final concentration of 50 or 75 nM, then 4 μl was applied to one side of a glow-discharged Quantifoil R2/2, 200 mesh, Cu/Rh grid. The grids were blotted on both sides and flash-frozen in liquid ethane by using a Vitrobot (FEI) at 4°C and 85%–100% humidity. Micrographs were recorded with low-dose conditions on a Tecnai F20 microscope, at 200 kV, a nominal magnification of 50,000×, and a defocus of 1.8–5.0 μm. Micrographs were digitized by using a KZA scanner (MRC, Cambridge) with a 6 μm step size. Pixels were binned 2 × 2 before data processing to give 2.4 Å/pixel.

For each complex, over 30,000 particles were manually selected with Ximdisp (Crowther et al., 1996). Contrast transfer function (CTF) parameters were determined for the particles in each micrograph with ctfit (Ludtke et al., 1999). Phase-flipped particles were used for iterative refinements by using the EMAN *refine* command (classification by projection matching, class averaging, and 3D reconstruction as described [Ludtke et al., 1999, 2004]) for each of the four independent datasets. As a starting model for all four structures, we used a 40S map derived from the 15 Å cryo-EM map of yeast 80S (kindly provided by Joachim Frank [Beckmann et al., 2001]), filtered to 60 Å prior to use. Importantly, similar results were obtained when a map derived from the *Thermus thermophilus* 30S crystal structure (Wimberly et al., 2000) filtered to 60 Å was used as the initial model (data not shown), suggesting that there is no significant model bias. The final resolutions of the reconstructions were estimated by using a Fourier Shell Correlation (FSC) value of 0.5. In an attempt to obtain higher-resolution maps, we used a large number of particles (over 30,000) for each reconstruction and also tried supervised classification to separate out alternative conformations. However, we were unable to obtain resolutions higher than 21–25 Å, likely due to structural flexibility of the small subunit (Gabashvili et al., 1999). We also note that similar resolutions could be obtained with fewer particles (~13,000). However, the 40S subunit has a preferred orientation in ice and including the larger number of particles ensured that all orientations were adequately represented.

Reconstructions were filtered to 20 Å. Figures were made with PyMOL (Delano Scientific; http://www.pymol.org), and maps were surface shaded at a contour level that encloses a density representing the mass of the 40S subunit (~1200 kDa where 50% is rRNA and 50% is protein). Difference densities were calculated in EMAN with maps filtered to 25 Å. The difference maps themselves were also filtered to 25 Å and are displayed at contour levels corresponding to +20 or −12 σ (where sigma is the number of standard deviations above the mean of the input map). For descriptions of additional tests to validate the significance of conformational changes, please refer to Supplemental Figure Legends. To aid analysis, a model of *S. cerevisiae* 40S (PDB 1S1H [Spahn et al., 2004a]) was manually placed in the density with Chimera (Goddard et al., 2006) and refined as a rigid structure by using Situs (Wriggers and Birmanns, 2001).

Kinetic Experiments

Ternary complex loading and dissociation was monitored by using a native gel shift assay as previously described (Lorsch and Herschlag, 1999; Algire et al., 2002). Buffer conditions were 30 mM HEPES-KOH (pH 7.4), 100 mM KOAc, 3 mM $Mg(OAc)_2$, and 2 mM DTT. Component concentrations were 0.5 nM ^{35}S-Met-$tRNA_i^{Met}$, 200 nM eIF2, 1 μM

eIF1, 1 μM eIF1A, and 4 μM mRNA. For k_{on} measurements, reactions were initiated by mixing preassembled ternary complex (all ternary complexes were made with GDPNP) with preassembled 40S•eIF1•eIF1A•mRNA complexes. Reactions were "stopped" by mixing with a 300-fold excess of unlabeled ternary complex. This prevents any further binding of labeled ternary complex to the ribosome. The extremely slow kinetics of ternary complex dissociation allows for ample time to load the reactions onto gels prior to significant dissociation of labeled ternary complex. k_{obs} was calculated by plotting the fraction of tRNA bound to the 40S subunit as a function of time and fitting the data with a single exponential. k_{on} was calculated by plotting k_{obs} as a function of 40S subunit concentration and fitting the data with a straight line ($k_{obs} = k_{on}[40S] + k_{off}$).

For k_{off} measurements, reactions were initiated by mixing preassembled 43S complexes (consisting of 40S subunits, labeled ternary complex, and the indicated factors and mRNA) with a 300-fold excess of unlabeled ternary complex. Reactions were stopped by loading onto a running native gel. k_{off} was calculated by plotting the fraction of labeled tRNA bound to the 40S subunit as a function of time and fitting the data with a single exponential. Control experiments indicate that the unlabeled ternary complex "chase" is stable for at least 2 days (data not shown). Degradation of 43S complexes becomes significant after 2 days (data not shown), making it difficult to accurately measure extremely slow rate constants such as that observed in the absence of eIF1 (Figure 4C).

Supplemental Data

Supplemental Data include Supplemental References, three figures, and five movies and are available with this article online at http://www.molecule.org/cgi/content/full/26/1/41/DC1/.

ACKNOWLEDGMENTS

We thank Richard Henderson for valuable discussions, advice on electron microscopy, and comments on the manuscript. We are grateful to Joachim Frank for providing a 15 Å cryo-EM map of the yeast 40S subunit and Shaoxia Chen, Alan Roseman, Peter Rosenthal, Jude Short, and Steve Ludtke for assistance with EM and image processing. We also thank Albert Weixlbaumer for useful discussions, Frank Murphy for providing a script to evaluate and sort data, and Junjie Zhang for providing EMAN scripts to calculate variance maps. This work was supported by the Medical Research Council (UK), the Agouron Institute and National Institute of Health grants GM67624 (to V.R.) and GM62128 (to J.R.L.). L.A.P. is a Beit Memorial Research Fellow, and T.M.S. was supported by a fellowship from EMBO and is funded by a Human Frontiers Science Program Organization long term fellowship.

Received: November 6, 2006
Revised: March 13, 2007
Accepted: March 26, 2007
Published: April 12, 2007

REFERENCES

Algire, M.A., Maag, D., Savio, P., Acker, M.G., Tarun, S.Z., Jr., Sachs, A.B., Asano, K., Nielsen, K.H., Olsen, D.S., Phan, L., et al. (2002). Development and characterization of a reconstituted yeast translation initiation system. RNA *8*, 382–397.

Algire, M.A., Maag, D., and Lorsch, J.R. (2005). Pi release from eIF2, not GTP hydrolysis, is the step controlled by start-site selection during eukaryotic translation initiation. Mol. Cell *20*, 251–262.

Antoun, A., Pavlov, M.Y., Lovmar, M., and Ehrenberg, M. (2006). How initiation factors tune the rate of initiation of protein synthesis in bacteria. EMBO J. *25*, 2539–2550.

Beckmann, R., Spahn, C.M., Eswar, N., Helmers, J., Penczek, P.A., Sali, A., Frank, J., and Blobel, G. (2001). Architecture of the protein-conducting channel associated with the translating 80S ribosome. Cell *107*, 361–372.

Bushell, M., and Sarnow, P. (2002). Hijacking the translation apparatus by RNA viruses. J. Cell Biol. *158*, 395–399.

Carter, A.P., Clemons, W.M., Jr., Brodersen, D.E., Morgan-Warren, R.J., Hartsch, T., Wimberly, B.T., and Ramakrishnan, V. (2001). Crystal structure of an initiation factor bound to the 30S ribosomal subunit. Science *291*, 498–501.

Chaudhuri, J., Chowdhury, D., and Maitra, U. (1999). Distinct functions of eukaryotic translation initiation factors eIF1A and eIF3 in the formation of the 40 S ribosomal preinitiation complex. J. Biol. Chem. *274*, 17975–17980.

Crowther, R.A., Henderson, R., and Smith, J.M. (1996). MRC image processing programs. J. Struct. Biol. *116*, 9–16.

Dallas, A., and Noller, H.F. (2001). Interaction of translation initiation factor 3 with the 30S ribosomal subunit. Mol. Cell *8*, 855–864.

Das, S., Ghosh, R., and Maitra, U. (2001). Eukaryotic translation initiation factor 5 functions as a GTPase-activating protein. J. Biol. Chem. *276*, 6720–6726.

Fekete, C.A., Applefield, D.J., Blakely, S.A., Shirokikh, N., Pestova, T., Lorsch, J.R., and Hinnebusch, A.G. (2005). The eIF1A C-terminal domain promotes initiation complex assembly, scanning and AUG selection in vivo. EMBO J. *24*, 3588–3601.

Frank, J., Zhu, J., Penczek, P., Li, Y., Srivastava, S., Verschoor, A., Radermacher, M., Grassucci, R., Lata, R.K., and Agrawal, R.K. (1995). A model of protein synthesis based on cryo-electron microscopy of the E. coli ribosome. Nature *376*, 441–444.

Gabashvili, I.S., Agrawal, R.K., Grassucci, R., and Frank, J. (1999). Structure and structural variations of the Escherichia coli 30 S ribosomal subunit as revealed by three-dimensional cryo-electron microscopy. J. Mol. Biol. *286*, 1285–1291.

Goddard, T.D., Huang, C.C., and Ferrin, T.E. (2006). Visualizing density maps with UCSF Chimera. J. Struct. Biol. *157*, 281–287.

Hershey, J.W.B., and Merrick, W.C. (2000). The Pathway and mechanism of initiation of protein synthesis. In Translational Control of Gene Expression, N. Sonenberg, J.W.B. Hershey, and M.B. Mathews, eds. (Cold Spring Harbor, New York: Cold Spring Harbor Laboratory Press), pp. 33–88.

Johnson, K.A. (1992). Transient-state kinetic analysis of enzyme reaction pathways. In The Enzymes, D. Sigman, ed. (San Diego, CA: Academic Press), pp. 1–61.

Kapp, L.D., and Lorsch, J.R. (2004a). GTP-dependent recognition of the methionine moiety on initiator tRNA by translation factor eIF2. J. Mol. Biol. *335*, 923–936.

Kapp, L.D., and Lorsch, J.R. (2004b). The molecular mechanics of eukaryotic translation. Annu. Rev. Biochem. *73*, 657–704.

Lata, K.R., Agrawal, R.K., Penczek, P., Grassucci, R., Zhu, J., and Frank, J. (1996). Three-dimensional reconstruction of the Escherichia coli 30 S ribosomal subunit in ice. J. Mol. Biol. *262*, 43–52.

Lomakin, I.B., Kolupaeva, V.G., Marintchev, A., Wagner, G., and Pestova, T.V. (2003). Position of eukaryotic initiation factor eIF1 on the 40S ribosomal subunit determined by directed hydroxyl radical probing. Genes Dev. *17*, 2786–2797.

Lorsch, J.R., and Herschlag, D. (1999). Kinetic dissection of fundamental processes of eukaryotic translation initiation in vitro. EMBO J. *18*, 6705–6717.

Ludtke, S.J., Baldwin, P.R., and Chiu, W. (1999). EMAN: semiautomated software for high-resolution single-particle reconstructions. J. Struct. Biol. *128*, 82–97.

Ludtke, S.J., Chen, D.H., Song, J.L., Chuang, D.T., and Chiu, W. (2004). Seeing GroEL at 6 A resolution by single particle electron cryomicroscopy. Structure *12*, 1129–1136.

Maag, D., and Lorsch, J.R. (2003). Communication between eukaryotic translation initiation factors 1 and 1A on the yeast small ribosomal subunit. J. Mol. Biol. *330*, 917–924.

Maag, D., Fekete, C.A., Gryczynski, Z., and Lorsch, J.R. (2005). A conformational change in the eukaryotic translation preinitiation complex and release of eIF1 signal recognition of the start codon. Mol. Cell *17*, 265–275.

Maag, D., Algire, M.A., and Lorsch, J.R. (2006). Communication between eukaryotic translation initiation factors 5 and 1A within the ribosomal pre-initiation complex plays a role in start site selection. J. Mol. Biol. *356*, 724–737.

Majumdar, R., Bandyopadhyay, A., and Maitra, U. (2003). Mammalian translation initiation factor eIF1 functions with eIF1A and eIF3 in the formation of a stable 40 S preinitiation complex. J. Biol. Chem. *278*, 6580–6587.

McCutcheon, J.P., Agrawal, R.K., Philips, S.M., Grassucci, R.A., Gerchman, S.E., Clemons, W.M., Jr., Ramakrishnan, V., and Frank, J. (1999). Location of translational initiation factor IF3 on the small ribosomal subunit. Proc. Natl. Acad. Sci. USA *96*, 4301–4306.

Olsen, D.S., Savner, E.M., Mathew, A., Zhang, F., Krishnamoorthy, T., Phan, L., and Hinnebusch, A.G. (2003). Domains of eIF1A that mediate binding to eIF2, eIF3 and eIF5B and promote ternary complex recruitment in vivo. EMBO J. *22*, 193–204.

Paulin, F.E., Campbell, L.E., O'Brien, K., Loughlin, J., and Proud, C.G. (2001). Eukaryotic translation initiation factor 5 (eIF5) acts as a classical GTPase-activator protein. Curr. Biol. *11*, 55–59.

Penczek, P.A., Yang, C., Frank, J., and Spahn, C.M. (2006). Estimation of variance in single-particle reconstruction using the bootstrap technique. J. Struct. Biol. *154*, 168–183.

Pestova, T.V., and Kolupaeva, V.G. (2002). The roles of individual eukaryotic translation initiation factors in ribosomal scanning and initiation codon selection. Genes Dev. *16*, 2906–2922.

Pestova, T.V., Borukhov, S.I., and Hellen, C.U. (1998). Eukaryotic ribosomes require initiation factors 1 and 1A to locate initiation codons. Nature *394*, 854–859.

Pestova, T.V., Kolupaeva, V.G., Lomakin, I.B., Pilipenko, E.V., Shatsky, I.N., Agol, V.I., and Hellen, C.U. (2001). Molecular mechanisms of translation initiation in eukaryotes. Proc. Natl. Acad. Sci. USA *98*, 7029–7036.

Pisarev, A.V., Kolupaeva, V.G., Pisareva, V.P., Merrick, W.C., Hellen, C.U., and Pestova, T.V. (2006). Specific functional interactions of nucleotides at key -3 and +4 positions flanking the initiation codon with components of the mammalian 48S translation initiation complex. Genes Dev. *20*, 624–636.

Schluenzen, F., Tocilj, A., Zarivach, R., Harms, J., Gluehmann, M., Janell, D., Bashan, A., Bartels, H., Agmon, I., Franceschi, F., and Yonath, A. (2000). Structure of functionally activated small ribosomal subunit at 3.3 angstroms resolution. Cell *102*, 615–623.

Singh, C.R., He, H., Ii, M., Yamamoto, Y., and Asano, K. (2004). Efficient incorporation of eukaryotic initiation factor 1 into the multifactor complex is critical for formation of functional ribosomal preinitiation complexes in vivo. J. Biol. Chem. *279*, 31910–31920.

Sonenberg, N., and Dever, T.E. (2003). Eukaryotic translation initiation factors and regulators. Curr. Opin. Struct. Biol. *13*, 56–63.

Spahn, C.M., Beckmann, R., Eswar, N., Penczek, P.A., Sali, A., Blobel, G., and Frank, J. (2001a). Structure of the 80S ribosome from Saccharomyces cerevisiae–tRNA-ribosome and subunit-subunit interactions. Cell *107*, 373–386.

Spahn, C.M., Kieft, J.S., Grassucci, R.A., Penczek, P.A., Zhou, K., Doudna, J.A., and Frank, J. (2001b). Hepatitis C virus IRES RNA-induced changes in the conformation of the 40s ribosomal subunit. Science *291*, 1959–1962.

Spahn, C.M., Gomez-Lorenzo, M.G., Grassucci, R.A., Jorgensen, R., Andersen, G.R., Beckmann, R., Penczek, P.A., Ballesta, J.P., and Frank, J. (2004a). Domain movements of elongation factor eEF2 and the eukaryotic 80S ribosome facilitate tRNA translocation. EMBO J. *23*, 1008–1019.

Spahn, C.M., Jan, E., Mulder, A., Grassucci, R.A., Sarnow, P., and Frank, J. (2004b). Cryo-EM visualization of a viral internal ribosome entry site bound to human ribosomes: the IRES functions as an RNA-based translation factor. Cell *118*, 465–475.

Valasek, L., Nielsen, K.H., Zhang, F., Fekete, C.A., and Hinnebusch, A.G. (2004). Interactions of eukaryotic translation initiation factor 3 (eIF3) subunit NIP1/c with eIF1 and eIF5 promote preinitiation complex assembly and regulate start codon selection. Mol. Cell. Biol. *24*, 9437–9455.

Wimberly, B.T., Brodersen, D.E., Clemons, W.M., Jr., Morgan-Warren, R.J., Carter, A.P., Vonrhein, C., Hartsch, T., and Ramakrishnan, V. (2000). Structure of the 30S ribosomal subunit. Nature *407*, 327–339.

Wriggers, W., and Birmanns, S. (2001). Using situs for flexible and rigid-body fitting of multiresolution single-molecule data. J. Struct. Biol. *133*, 193–202.

Yoon, H.J., and Donahue, T.F. (1992). The suil suppressor locus in Saccharomyces cerevisiae encodes a translation factor that functions during tRNA(iMet) recognition of the start codon. Mol. Cell. Biol. *12*, 248–260.

Yusupova, G.Z., Yusupov, M.M., Cate, J.H., and Noller, H.F. (2001). The path of messenger RNA through the ribosome. Cell *106*, 233–241.

Accession Numbers

The apo 40S, 40S-eIF1-eIF1A, 40S-eIF1, and 40S-eIF1A cryo-EM maps have been deposited in the 3D EM database with accession codes EMD-1346, EMD-1347, EMD-1348, and EMD-1349, respectively.